BRAIN COMMUNICATIONS

Objective biomarkers for clinical relapse in multiple sclerosis: a metabolomics approach

Tianrong Yeo,[1,2,3] Fay Probert,[1] Megan Sealey,[1] Luisa Saldana,[4] Ruth Geraldes,[4] Sebastian Höckner,[5] Eric Schiffer,[5] Timothy D.W. Claridge,[6] David Leppert,[7] Gabriele DeLuca,[4] Jens Kuhle,[7] Jacqueline Palace[4] and Daniel C. Anthony[1]

Accurate determination of relapses in multiple sclerosis is important for diagnosis, classification of clinical course and therapeutic decision making. The identification of biofluid markers for multiple sclerosis relapses would add to our current diagnostic armamentarium and increase our understanding of the biology underlying the clinical expression of inflammation in multiple sclerosis. However, there is presently no biofluid marker capable of objectively determining multiple sclerosis relapses although some, in particular neurofilament-light chain, have shown promise. In this study, we sought to determine if metabolic perturbations are present during multiple sclerosis relapses, and, if so, identify candidate metabolite biomarkers and evaluate their discriminatory abilities at both group and individual levels, in comparison with neurofilament-light chain. High-resolution global and targeted ^{1}H nuclear magnetic resonance metabolomics as well as neurofilament-light chain measurements were performed on the serum in four groups of relapsing-remitting multiple sclerosis patients, stratified by time since relapse onset: (i) in relapse (R); (ii) last relapse (LR) $\geq$ 1 month (M) to $<$ 6 M ago; (iii) LR $\geq$ 6 M to $<$ 24 M ago; and (iv) LR $\geq$ 24 M ago. Two hundred and one relapsing-remitting multiple sclerosis patients were recruited: R (n = 38), LR 1–6 M (n = 28), LR 6–24 M (n = 34), LR $\geq$ 24 M (n = 101). Using supervised multivariate analysis, we found that the global metabolomics profile of R patients was significantly perturbed compared to LR $\geq$ 24 M patients. Identified discriminatory metabolites were then quantified using targeted metabolomics. Lysine and asparagine (higher in R), as well as, isoleucine and leucine (lower in R), were shortlisted as potential metabolite biomarkers. ANOVA of these metabolites revealed significant differences across the four patient groups, with a clear trend with time since relapse onset. Multivariable receiver operating characteristics analysis of these four metabolites in discriminating R versus LR $\geq$ 24 M showed an area under the curve of 0.758, while the area under the curve for serum neurofilament-light chain was 0.575. Within individual patients with paired relapse–remission samples, all four metabolites were significantly different in relapse versus remission, with the direction of change consistent with that observed at group level, while neurofilament-light chain was not discriminatory. The perturbations in the identified metabolites point towards energy deficiency and immune activation in multiple sclerosis relapses, and the measurement of these metabolites, either singly or in combination, are useful as biomarkers to differentiate relapse from remission at both group and individual levels.

1 Department of Pharmacology, University of Oxford, Oxford OX1 3QT, UK
2 Department of Neurology, National Neuroscience Institute, Singapore 308433, Singapore
3 Duke-NUS Medical School, Singapore 169857, Singapore
4 Nuffield Department of Clinical Neurosciences, John Radcliffe Hospital, University of Oxford, Oxford OX3 9DU, UK
5 numares AG, Regensburg 93053, Germany
6 Chemistry Research Laboratory, Department of Chemistry, University of Oxford, Oxford OX1 3TA, UK
7 Neurologic Clinic and Policlinic, MS Center and Research Center for Clinical Neuroimmunology and Neuroscience Basel (RC2NB), Departments of Biomedicine and Clinical Research, University Hospital Basel and University of Basel, Basel CH-4031, Switzerland

Received June 30, 2021. Revised September 01, 2021. Accepted September 21, 2021. Advance Access publication October 12, 2021

Correspondence to: Jacqueline Palace, FRCP, DM
Nuffield Department of Clinical Neurosciences, University of Oxford, Level 6, West Wing
John Radcliffe Hospital, OX3 9DU, Oxford, UK
E-mail: jacqueline.palace@ndcn.ox.ac.uk

Correspondence may also be addressed to: Daniel C. Anthony, PhD
Department of Pharmacology, University of Oxford, Mansfield Road, OX1 3QT, Oxford, UK
E-mail: daniel.anthony@pharm.ox.ac.uk

Keywords: multiple sclerosis; relapse; metabolomics; metabolites; biomarker

Abbreviations: AU = arbitrary units; AUC = area under the curve; BBB = blood brain barrier; BCAA = branched-chain amino acid; BMI = body mass index; 95% CI = 95% confidence interval; CPMG = Carr–Purcell–Meiboom–Gill; DMT = disease modifying therapy; EAE = experimental autoimmune encephalomyelitis; EDSS = expanded disability status scale; GAD = gadolinium; HDL = high-density lipoprotein; LDL = low-density lipoprotein; LR 1–6 M = last relapse ≥ 1 month to < 6 months ago; LR 6–24 M = last relapse ≥ 6 months to < 24 months ago; LR ≥ 24 M = last relapse ≥ 24 months ago; MBP = myelin basic protein; mTOR = mammalian target of rapamycin; NfL = neurofilament-light chain; NMOSD = neuromyelitis optica spectrum disorder; NMR = nuclear magnetic resonance; OPLS-DA = orthogonal partial-least squares determinant analysis; ppm = parts per million; R = in relapse; ROC = receiver operating characteristics; RRMS = relapsing-remitting multiple sclerosis; SD = standard deviation; TOCSY = total correlation spectroscopy; VIP = variable importance in projection

Graphical Abstract

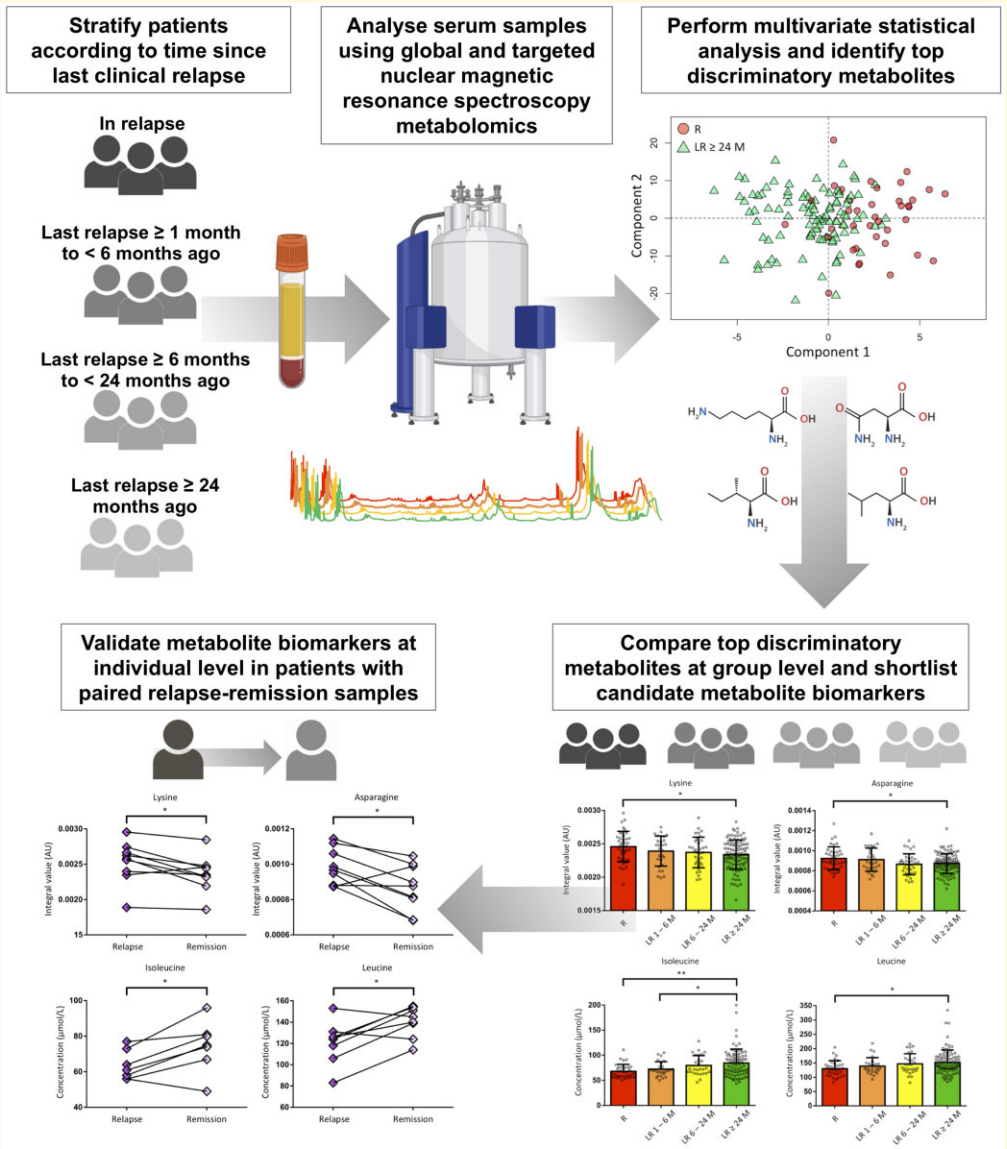

Introduction

Accurate determination of relapses in multiple sclerosis is important for diagnosis, classification of clinical course and therapeutic decision making. To date, the history and neurological examination of a patient, as compared to previous examinations, are the principal methods used to establish relapses. This is often supplemented by MRI where the presence of gadolinium (GAD)-enhancing or new/enlarging T_2 lesion/s consistent with the neurological deficits offers supportive evidence for diagnosing relapses. However, a clinico-radiological discordance is often encountered at the time of a relapse, which is, in part, contributed by the limited sensitivity of conventional MRI to detect small lesions, particularly in the spinal cord, cortical grey matter and optic nerve.[1–3] There is a need to understand the biology underlying the clinical expression of the inflammatory attack, and also, to measure it objectively in biofluids so as to discover biomarkers of multiple sclerosis relapses. Although none are as yet used in routine clinical practice, some biofluid markers show promise especially neurofilament-light chain (NfL), which, is observed to be elevated during relapses compared to remission in several publications and in a recent meta-analysis,[4–9] and has also been reported to be able to predict and monitor future disease activity.[10,11]

Clinical metabolomics is the comprehensive investigation of low molecular weight (< 1500 Da) metabolites within a biological sample and is emerging as a useful downstream 'omics' platform for biomarker discovery and in the understanding of disease pathophysiology.[12] Our previous work on metabolomics in neuroinflammatory diseases showed that metabolites can function as diagnostic and prognostic biomarkers by: (i) distinguishing multiple sclerosis from aquaporin-4-antibody disease and myelin oligodendrocyte glycoprotein-antibody disease accurately[13]; (ii) aiding in the classification of patients with overlapping features of multiple sclerosis and neuromyelitis optica spectrum disorder[14]; (iii) predicting clinical conversion of clinically isolated syndrome to multiple sclerosis[15]; and (iv) distinguishing relapsing-remitting multiple sclerosis (RRMS) from secondary progressive multiple sclerosis with high accuracy.[16,17] With regards to the application of metabolomics in the context of multiple sclerosis relapses, two studies have reported metabolic perturbations in CSF during relapses compared to remission.[18,19] However, this was not the primary objective in both studies, which also had modest sample sizes (range, 50–54 multiple sclerosis patients) and the use of CSF precludes frequent sampling in the clinical setting.

In this study, we sought to determine if ^{1}H nuclear magnetic resonance (NMR) metabolomics using serum could distinguish RRMS patients in relapse from those in remission, and, if so, identify metabolite biomarkers for relapses that are informative at both group and individual levels. First, we assessed whether global metabolomics perturbations are present in patients in relapse compared to those in stable remission (i.e. no relapse in the last 2 years), and, if present, we determined the duration of this metabolic derangement. Next, we selected the top discriminatory metabolites distinguishing patients in relapse from those in stable remission and quantified the metabolites using targeted metabolomics. We evaluated the shifts (i.e. increasing or decreasing) in the top discriminatory metabolites in a larger group of patients, stratified by time since the onset of relapse. Consistent shifts across the patient groups were found to support the use of these metabolites as potential biomarkers of relapse. We then determined whether these metabolites could be discriminatory at an individual level in patients having paired relapse–remission samples. Lastly, we sought to compare the discriminatory abilities of the identified metabolite biomarkers against serum NfL for distinguishing patients in relapse from those in remission at both group and individual levels.

Materials and methods

Patients

RRMS patients were prospectively recruited from the John Radcliffe Hospital, Oxford University Hospital Trust, consented under the Oxford Radcliffe Biobank and approved by the NRES Committee South Central—Oxford C (REC reference: 09/H0606/5 + 5). All patients fulfilled the 2017 revisions to the McDonald criteria for multiple sclerosis.[20] Patients with symptoms suggestive of a relapse were first triaged by an experienced multiple sclerosis nurse via phone consultation and those suspected to have a relapse were then seen at the 'relapse' clinic. Relapse status was established by multiple sclerosis neurologists and defined clinically in accordance with the 2017 McDonald criteria—a monophasic clinical episode with patient-reported symptoms and objective findings typical of multiple sclerosis, reflecting a focal or multifocal inflammatory demyelinating event in the CNS, developing acutely or subacutely, with a duration of at least 24 h, with or without recovery, and in the absence of fever or infection.[20] Patients with pseudo-relapses were excluded by performing a systematic review of infective symptoms, temperature measurement, and urine dipstick to evaluate for urinary tract infection. Detailed clinical, MRI and demographic data were collected at the time of recruitment.

Patients were divided into four groups according to the interval between their last relapse to blood sampling: (i) in relapse, defined as $<$ 1 month from the onset of first symptom/s of relapse; (ii) last relapse (LR) $\geq$ 1 month to $<$ 6 months ago; (iii) LR $\geq$ 6 months to $<$ 24 months ago; and (iv) LR $\geq$ 24 months ago. These groups are henceforth referred to as 'R', 'LR 1–6 M', 'LR 6–24 M' and 'LR $\geq$ 24 M', respectively.

Blood collection

A validated, optimized blood collection protocol for serum metabolomics was employed.[16] Blood was collected in vacutainer tubes (BD 367837), left to stand for 30 min, and then centrifuged at 1300 $\times g$ for 10 min at room temperature. Serum was then immediately aliquoted and stored at −80°C until NMR experimentation.

Global metabolomics

Global metabolomics detects all measurable metabolites in a sample and is ideal for comprehensive biochemical profiling for biomarker discovery. All ^{1}H NMR experiments for global metabolomics were performed at the Department of Chemistry, University of Oxford, using a 700-MHz Bruker AVIII spectrometer, with the Carr–Purcell–Meiboom–Gill (CPMG) relaxation editing pulse sequence for spectra acquisition. Technical details of NMR sample preparation, experiments and spectra processing have been previously published.[13,16] Integral values of individual spectral 'bins' were computed with constant-sum-normalization and used as quantitative variables expressed in arbitrary units (AU). In all, 191 metabolite 'bins' were available for multivariate statistical analysis. Metabolite assignments were performed by referencing to literature values and the Human Metabolome Database,[21] as well as inspection of the 1D total correlation spectroscopy spectra.

Targeted metabolomics

Targeted metabolomics detects pre-defined chemical groups and known metabolites, and is optimized for focussed measurements with absolute quantification. Targeted metabolomics was performed with the *AXINON® lipoFIT®* test for advanced lipoprotein analysis on the standardized *AXINON®* system at numares AG, Regensburg, Germany, using a 600-MHz Bruker AVIII ^{1}H NMR spectrometer with the zgpr30 pulse sequence for spectra acquisition as previously described.[22] This test system deconvolutes the broad methyl lipoprotein NMR resonance into its constituent parts, allowing for the absolute quantification of the cholesterol content, number of particles and mean particle diameter of each lipoprotein subpopulation.[23] The test system also provides absolute quantification of metabolites whose NMR resonances partially overlap with the lipoprotein resonances. These metabolites include lactate, glucose, alanine and the branched-chain amino acids (BCAAs)—isoleucine, leucine and valine. In all, 29 parameters were available for multivariate statistical analysis.

Serum NfL level determination

Serum NfL levels were measured using the Simoa® assay (NF-LIGHT, Quanterix) performed at the University of Basel, Switzerland. Assay techniques and principles have been previously described.[9]

Multivariate statistical analysis

Orthogonal partial-least squares discriminant analysis (OPLS-DA) using in-house R scripts (R foundation for statistical computing, Vienna, Austria) and the *ropls* package were used to interrogate the CPMG (global metabolomics) and *AXINON® lipoFIT®* (targeted metabolomics) spectral data to identify metabolomics differences between patient groups.[24,25] All OPLS-DA models were validated on independent test data using external 10-fold cross-validation with 100 iterations. Details of this approach have been previously published.[13] Briefly, this involves repeated cycles of (i) balancing class sizes; (ii) random splitting of the spectral data into a training set (90% of data) and a test set (remaining 10% of data); (iii) construction of OPLS-DA models using the training set alone; and then (iv) determining the predictive accuracy of the OPLS-DA model using the independent test set. The validity of the metabolic separation between patient groups was confirmed if the mean predictive accuracy of the ensemble of model accuracies was significantly higher than the mean predictive accuracy of a separate ensemble created by random class assignments on the same spectral data.

Univariable and multivariable statistical analysis

Analysis of demographic, clinical and metabolite data was performed using STATA (release 14) and GraphPad Prism (version 6). Comparative analyses between patient groups were performed using one-way ANOVA or Kruskal–Wallis test as appropriate for continuous variables, with pair-wise *post-hoc* corrections using Bonferroni and Dunn tests, respectively. Chi-square or Fisher exact tests were used for categorical variables as appropriate, with Bonferroni correction when comparing ≥ 3 groups. Pearson or Spearman correlation was used to explore correlations depending on data normality. Area under the curve (AUC) was obtained using receiver operating characteristics (ROC) analysis. Two-tailed P-values of < 0.05 were considered statistically significant and data were presented as mean ± standard deviation (SD) unless stated otherwise.

Data availability

Anonymized data and code will be shared by request from any qualified investigator.

Results

Patient characteristics

A total of 201 RRMS patients were recruited: R ($n = 38$), LR 1–6 M ($n = 28$), LR 6–24 M ($n = 34$) and LR ≥ 24

M ($n = 101$). Demographic and clinical characteristics are shown in Table 1.

The R and LR 1–6 M patients were younger and fewer were on disease modifying therapy (DMT), compared to LR $\geq$ 24 M patients. More R patients had steroid use ($n = 5$) compared to LR $\geq$ 24 M patients, although all patients had already completed steroids in the past 1 week before blood sampling. Expectedly, expanded disability status scale (EDSS) of R patients was higher compared to the other three groups. A higher proportion of LR 1–6 M patients had evidence of MRI activity (new T_2 and/or GAD-enhancing lesion/s) compared to LR $\geq$ 24 M patients. This reflected clinical practices as clinicians were more likely to perform MRI in patients after being seen in the 'relapse' clinic, with the MRI done a few weeks later, whilst clinicians were less likely to perform frequent/GAD-contrasted scans in LR $\geq$ 24 M patients. While not all R patients had MRI performed contemporaneous with their relapse, 6 of 24 (25%) had GAD-enhancing lesion/s and 8 of 19 (42.1%) had new T_2 lesion/s (referenced to a baseline scan done within one year) on MRI performed within the next 6 months after relapse onset.

Global metabolomics

R versus LR $\geq$ 24 M patients

To identify global metabolomics perturbations reflective of clinical relapses, OPLS-DA was used to construct discriminatory models using CPMG spectral data to distinguish between R and LR $\geq$ 24 M patients. The representative OPLS-DA scores plot showed a moderate separation between R and LR $\geq$ 24 M patients (Fig. 1A). The mean predictive accuracy for the ensemble of the OPLS-DA models of R versus LR $\geq$ 24 M patients was significantly higher than the mean predictive accuracy of the ensemble created by random class assignments ($62.6\% \pm 4.8\%$ versus $50.9\% \pm 8.2\%$; $P < 0.0001$) (Fig. 1B), validating the metabolomics differences between these two patient groups.

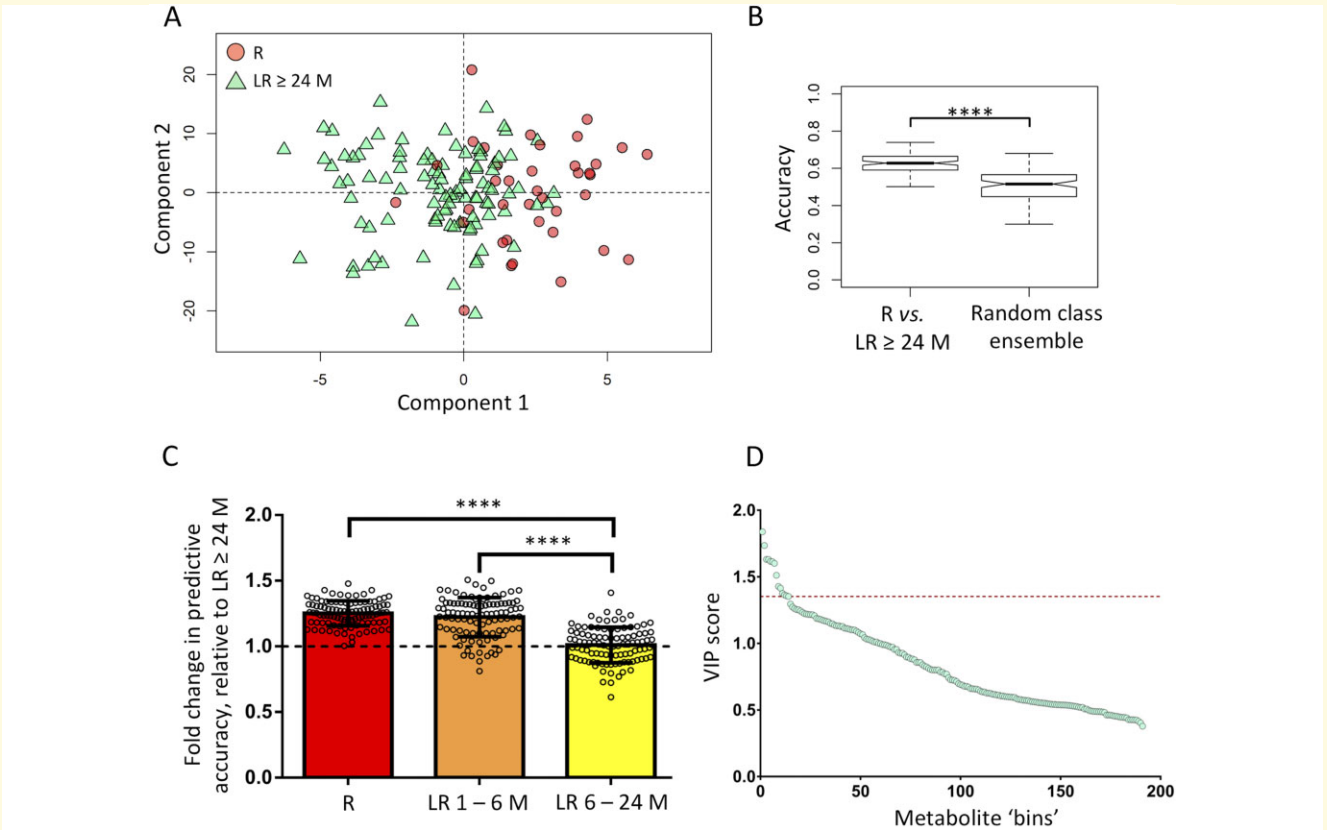

Figure 1 Global metabolomics. (**A**) Representative scores plot from the OPLS-DA models of R versus LR $\geq$ 24 M patients (R = red circles, LR $\geq$ 24 M = green triangles). (**B**) Box plots of predictive accuracies, against random class assignment. **** indicates $P < 0.0001$ by Kolmogorov–Smirnov test. (**C**) Fold change in predictive accuracies of the OPLS-DA models of the different patient groups with respect to the reference comparator, i.e. LR $\geq$ 24 M patients. The fold change of random chance is 1.0 as indicated by the dashed horizontal line. **** indicates $P < 0.0001$ by *post-hoc* Bonferroni correction. (**D**) VIP score ranking plot obtained from the OPLS-DA models of R versus LR $\geq$ 24 M patients. The dashed red line indicates the VIP score threshold of 1.35, before a 'drop-off' in VIP score. Metabolites with VIP scores above this cut-off are detailed in Table 2. LR 1–6 M = last relapse $\geq$ 1 month to $<$ 6 months ago; LR 6–24 M = last relapse $\geq$ 6 months to $<$ 24 months ago; LR $\geq$ 24 M = last relapse $\geq$ 24 months ago; OPLS-DA = orthogonal partial-least squares determinant analysis; R = in relapse; VIP = variable importance in projection.

Table 1 Demographic and clinical details of the study population

	R ($n = 38$)	LR 1–6 M ($n = 28$)	LR 6–24 M ($n = 34$)	LR ≥ 24 M ($n = 101$)	*P*-value across groups
Age in years, mean (SD)	38.3 (9.5)[a]	38.7 (7.0)[b]	43.5 (9.7)	44.2 (9.9)[a,b]	0.002
Female, no. (%)	27 (71.1)	23 (82.1)	22 (64.7)	73 (72.3)	0.503
White ethnicity, no. (%)	37 (97.4)	25 (89.3)	31 (91.2)	92 (91.1)	0.589
Recent/current steroid use, no. (%)	5 (13.2)[a]	0 (0.0)	1 (2.9)	1 (1.0)[a]	0.011
DMT use, no. (%)	18 (47.4)[a]	12 (42.9)[b]	20 (58.8)	75 (74.3)[a,b]	0.002
Alemtuzumab	1 (5.6)	1 (8.3)	1 (5.0)	2 (2.7)	
Dimethyl fumarate	6 (33.3)	2 (16.7)	6 (30.0)	13 (17.3)	
Fingolimod	2 (11.1)	2 (16.7)	2 (10.0)	10 (13.3)	
Glatiramer acetate	6 (33.3)	5 (41.7)	7 (35.0)	25 (33.3)	
Interferons	1 (5.6)	0 (0.0)	3 (15.0)	18 (24.0)	
Natalizumab	1 (5.6)	2 (16.7)	1 (5.0)	5 (6.7)	
Teriflunomide	1 (5.6)	0 (0.0)	0 (0.0)	2 (2.7)	
EDSS, median (range)	3.3 (1–7)[a,c,d]	2.5 (1–6.5)[c]	2.3 (0–8.5)[d]	2.0 (0–7)[a]	< 0.001
Disease duration in years, median (range)	11.1 (0.73–28.7)	7.5 (0.19–28.3)[b]	4.4 (0.54–28.5)[e]	12.1 (2.3–47.3)[b,e]	< 0.001
No comorbidities, no. (%)	16 (42.1)	10 (35.7)	8 (23.5)	42 (41.6)	0.271
Presence of new T_2 lesion/s within last 1 year, referenced to a baseline scan done ≤ 1 year apart, no. (%)	5/12 (41.7)	7/8 (87.5)[b]	4/9 (44.4)	3/22 (13.6)[b]	0.002
Presence of GAD-enhancing lesion/s within last 1 year, no. (%)	5/16 (31.3)	7/11 (63.6)[b]	4/12 (33.3)	1/21 (4.8)[b]	0.003
BMI, median (range)	26.5 (20–49)	25.0 (19–38.7)	27.0 (19.8–57.4)	24.8 (15–42)	0.081
Current smoker, no. (%)	5 (13.2)	5 (17.9)	3 (8.8)	12 (11.9)	0.751
Alcohol intake in units/week, median (range)	0 (0–16)	1.5 (0–35)	0 (0–18)	1 (0–24)	0.394
Time from last meal in hours, median (range)	3.7 (1.3–18.5)	3.6 (0.8–20.9)	3.6 (0.4–16.3)	3.3 (0.9–16.7)	0.319

P-values within the right most column indicate differences across the four groups of patients. Symbols indicate $P < 0.05$ for pair-wise comparison after *post-hoc* correction using Bonferroni or Dunn tests as appropriate. Recent steroid use is defined as steroid use within 1 month of blood sampling.
[a]R versus LR ≥ 24 M.
[b]LR 1–6 M versus LR ≥ 24 M.
[c]R versus LR 1–6 M.
[d]R versus LR 6–24 M.
[e]LR 6–24 M versus LR ≥ 24 M.
BMI = body mass index; DMT = disease modifying therapy; EDSS = expanded disability status scale; GAD = gadolinium; LR 1–6 M = last relapse ≥ 1 month to < 6 months ago; LR 6–24 M = last relapse ≥ 6 months to < 24 months ago; LR ≥ 24 M = last relapse ≥ 24 months ago; R = in relapse.

LR 1–6 M versus LR ≥ 24 M patients, and LR 6–24 M versus LR ≥ 24 M patients

To explore how long global metabolomics perturbations persist after relapses, OPLS-DA models were constructed using CPMG spectral data for LR 1–6 M as well as for LR 6–24 M patients against the reference comparator, i.e. LR ≥ 24 M patients. The mean predictive accuracy for the ensemble of the OPLS-DA models for LR 1–6 M versus LR ≥ 24 M patients was significantly higher than that of the random class ensemble (61.2% ± 7.5% versus 48.8% ± 8.5%; $P < 0$ 0.0001). In contrast, the mean accuracy of the OPLS-DA models for LR 6–24 M versus LR ≥ 24 M patients was not different from that of the random class ensemble (50.5% ± 6.7% versus 50.6% ± 7.8%; $P = 0.971$). The fold change in the predictive accuracy (normalized to the accuracy of random chance, i.e. 50%) of each patient group, using LR ≥ 24 M patients as reference comparator, is shown in Fig. 1C. Taking these findings in totality, this implies that global metabolomics perturbations persist for at least 6 months after a clinical relapse.

Identifying discriminatory metabolites from the R versus LR ≥ 24 M OPLS-DA models

To identify the top discriminatory metabolites from global metabolomics driving the distinction between R versus LR ≥ 24 M patients, variable importance in projection (VIP) scores were generated. The VIP score is a measure of the importance of a metabolite in the OPLS-DA model—the higher the VIP score, the greater the contribution a metabolite makes to the model.[25] The VIP score cut-off at 1.35 was determined by identifying a 'drop-off' on the VIP ranking plot (Fig. 1D). Metabolites with VIP scores above this cut-off are detailed in Table 2. These consisted predominantly of lipoproteins, amino acids and glucose. As two-thirds of these discriminatory metabolites are covered by the *AXINON*® *lipoFIT*® system, targeted metabolomics was performed next.

Targeted metabolomics

R versus LR ≥ 24 M patients

To investigate if metabolomics perturbations observed in relapses can be confirmed by targeted metabolomics,

Table 2 Top discriminatory metabolites from global metabolomics distinguishing R versus LR ≥ 24 M patients

Discriminatory metabolites	Chemical shift of contributing spectral 'bins' (VIP score, VIP rank)
Mobile $(-CH_3-)_n$ HDL/LDL[a]	0.84. . ..0.86 ppm (1.36, 12)
	0.86. . ..0.88 ppm (1.62, 5)
Leucine[a]	0.96. . ..0.98 ppm (1.36, 13)
Mobile $(-CH_2-)_n$ LDL[a]	1.22. . ..1.24 ppm (1.43, 9)
	1.24. . ..1.26 ppm (1.74, 2)
Lysine	1.40. . ..1.42 ppm (1.61, 6)
	1.42. . ..1.44 ppm (1.51, 8)
βCH_2[a]	1.62. . ..1.64 ppm (1.63, 3)
$/=CH-CH_2-CH_2-$[a]	1.96. . ..1.98 ppm (1.63, 4)
	1.98. . ..2.00 ppm (1.84, 1)
Asparagine	2.84. . ..2.86 ppm (1.41, 10)
Glucose[a]	3.88. . ..3.90 ppm (1.38, 11)
Phenylalanine (meta-)	7.42. . ..7.44 ppm (1.60, 7)

[a]Indicates metabolites accessible for absolute quantification using the *AXINON® lipoFIT®* system (targeted metabolomics).
HDL = high-density lipoprotein; LDL = low-density lipoprotein; LR ≥ 24 M = last relapse ≥ 24 months ago; ppm = parts per million; R = in relapse; VIP = variable importance in projection.

OPLS-DA was performed on the *AXINON® lipoFIT®* parameters obtained from R and LR ≥ 24 M patients. The mean predictive accuracy for the ensemble of the OPLS-DA models of R versus LR ≥ 24 M patients was significantly higher than that of the random class ensemble (58.1% ± 5.5% versus 50.5% ± 7.0%; $P < 0.0001$), confirming the presence of targeted metabolomics differences.

Identifying discriminatory metabolites from the R versus LR ≥ 24 M OPLS-DA models

VIP scores from the R versus LR ≥ 24 M OPLS-DA models were generated to elucidate the principal discriminatory metabolites from targeted metabolomics. The VIP ranking plot revealed isoleucine and leucine (both BCAAs) as the two most important metabolites (Fig. 2A), with VIP scores of 2.05 and 2.01, respectively. Isoleucine was not identified as one of the principal discriminatory metabolites on global metabolomics although it was the top discriminatory metabolite in targeted metabolomics. This is likely due to its NMR resonances overlapping with the broad, partly suppressed methyl lipoprotein signal in the CPMG spectra, thus masking its signal (Fig. 2B). In comparison, while the resonances from leucine also overlap with the broad lipoprotein signal, its integral value is greater as this comprise of signals arising from six ^1H nuclei (2x CH_3), hence enhancing its detection.

Exploring potential metabolite biomarkers of clinical relapses

The top discriminatory metabolites from targeted (isoleucine and leucine) and global metabolomics (metabolites listed in Table 2 not measured by targeted metabolomics) distinguishing R versus LR ≥ 24 M patients were shortlisted as potential metabolite biomarkers of relapses. One-way ANOVA was performed for each of these shortlisted metabolites across the four patient groups, using LR ≥ 24 M patients as the reference group. The workflow for choosing the candidate metabolites for ANOVA is illustrated in Fig. 3.

Lysine and asparagine (from global metabolomics), as well as isoleucine and leucine (from targeted metabolomics) were significant on one-way ANOVA. Both lysine and asparagine were higher in R compared to LR ≥ 24 M patients, and showed a decreasing trend with time away from relapse (Fig. 4A and B). The converse was observed for isoleucine and leucine—lower levels in R compared to LR ≥ 24 M patients and increasing over time (Fig. 4C and D). Taking these observations in totality, the measurements of lysine, asparagine, isoleucine and leucine are highlighted as potential metabolite biomarkers of clinical relapses.

On ROC analysis to distinguish R and LR ≥ 24 M patients, the univariable AUC of the four metabolite biomarkers ranged from 0.610 to 0.697 (Fig. 4E–H). The combination of the four metabolites as independent variables in a multivariable logistic regression model followed by ROC analysis resulted in an improved AUC of 0.758 (Fig. 4I).

Exploring serum NfL as a potential biomarker of clinical relapses

Serum NfL is a promising biomarker for inflammation-driven neuro-axonal injury and is elevated in clinical relapses, thus, its diagnostic performance in our cohort of patients was explored. One-way ANOVA of serum NfL levels, using LR ≥ 24 M patients as the reference group, showed that R patients had higher levels of serum NfL compared to LR ≥ 24 M patients (Fig. 5A). ROC analysis showed an AUC of 0.575 ($P = 0.176$) for serum NfL in distinguishing R versus LR ≥ 24 M patients (Fig. 5B). Next, we explored the combination of the four identified metabolites and NfL to improve the ability to distinguish R and LR ≥ 24 M patients. A multivariable logistic regression ROC analysis showed a modest increase in the AUC to 0.789 (Fig. 5C), as compared to using the four metabolites alone.

Evaluating metabolites as individualized, responsive biomarkers of clinical relapses

From the previous sections, lysine, asparagine, isoleucine and leucine were identified to be promising metabolite biomarkers of relapses at group level. However, for a biomarker to be clinically useful, it needs to be applicable in an individualized manner, and be sufficiently

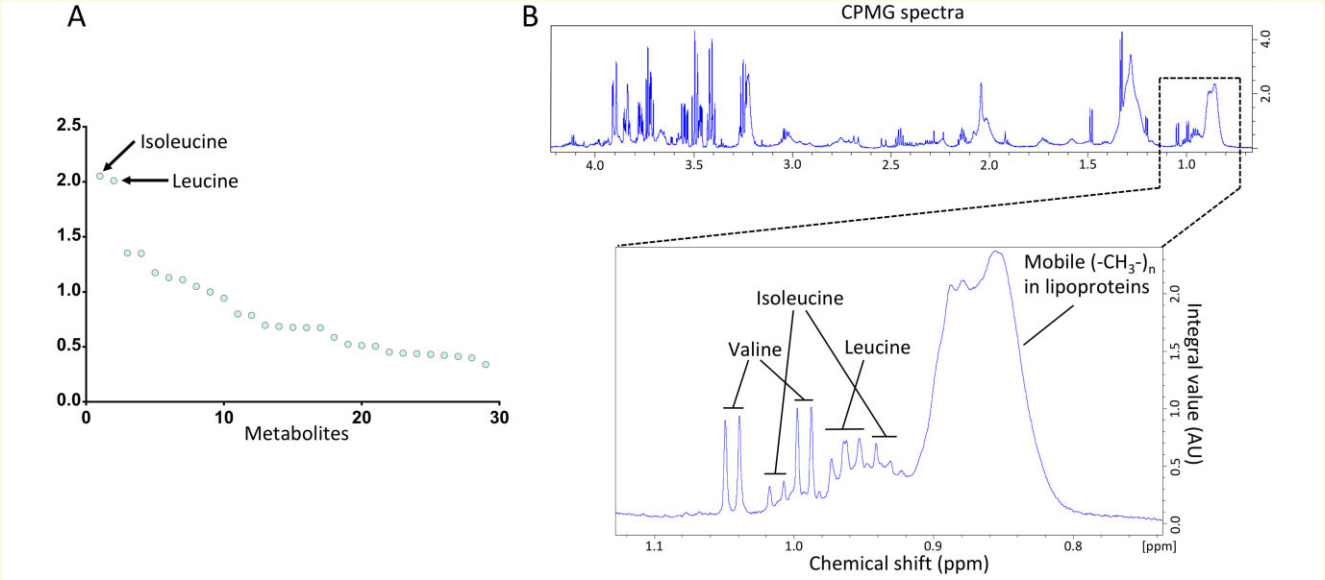

Figure 2 Identification of isoleucine and leucine as discriminatory metabolites. (**A**) VIP score ranking plot obtained from the OPLS-DA models of R versus LR ≥ 24 M patients on targeted metabolomics identifies isoleucine and leucine as the top two discriminatory metabolites. (**B**) BCAAs ^{1}H NMR resonances in CPMG-edited spectra (global metabolomics). The zoom in panel shows that the resonances from isoleucine (a triplet centred at 0.941 ppm arising from three ^{1}H nuclei and a doublet centred at 1.012 ppm also arising from three ^{1}H nuclei) overlap with the broad methyl $(-CH_3-)_n$ lipoprotein resonance, thus, attenuating its signal. Leucine resonances (two CH_3 doublets clustered at 0.963 ppm) also overlap with the lipoprotein signal, however, its integral value is greater (as compared to isoleucine) as this is derived from six ^{1}H nuclei (note the taller and broader signals compared to isoleucine), thus, the signal is more apparent despite the masking effect of the broad lipoprotein signal. AU = arbitrary units; BCAAs = branched-chain amino acids; CPMG = Carr–Purcell–Meiboom–Gill; LR ≥ 24 M = last relapse ≥ 24 months ago; NMR = nuclear magnetic resonance; OPLS-DA = orthogonal partial-least squares determinant analysis; ppm = parts per million; R = in relapse; VIP = variable importance in projection.

responsive such that the change in its levels between disease states is observable within a clinically useful time frame.

Nine patients (within the R group) who had paired relapse–remission samples (i.e. relapse first followed by remission), and with the remission sample collected within 6 months of relapse onset were identified. Median EDSS at relapse blood sampling was 4.0, decreasing to 2.5 at remission sampling, and, the median duration between relapse onset and remission sampling was 3.6 months (range, 2.3–5.6). It is of note that none of these nine patients had received steroids at the time of relapse blood sampling.

Paired *t*-testing revealed that all four metabolites exhibited significant differences in their levels in relapse and in remission (Fig. 6A–D), and, the direction of change was consistent with that observed at group level. There was no significant difference in serum NfL levels within this 6-month time frame (Fig. 6E). Of these nine patients, five had concordance in the direction of change for all four metabolites, three had discordance in one metabolite while one had disagreement for two metabolites. Given these observations, the four metabolites were combined in a multivariable ROC analysis to determine if a composite biomarker could improve discriminatory accuracy. An AUC of 0.911 (95% CI 0.728–1.000; $P < 0.001$) was achieved, while the addition of serum NfL did not improve accuracy (AUC = 0.896, 95% CI 0.683–1.000; $P < 0.001$).

Addressing potential confounders for the identified metabolite biomarkers

As shown in Table 1, several baseline characteristics were different across the four patient groups—notably age, steroid use and DMT use were dissimilar between R versus LR ≥ 24 M patients on *post-hoc* analysis. Two approaches were used to address these potential confounders: (i) for quantitative variables, correlation of the potential confounding variable with each of the four identified metabolite biomarkers was performed; and (ii) for categorical variables, the levels of the four metabolites were explored stratified by the potential confounding variable.

There were no correlations between any of the four metabolite biomarkers with age, EDSS and disease duration across the entire cohort of patients ($n = 201$). There were also no differences in any of the metabolite concentrations stratified by steroid use in the whole

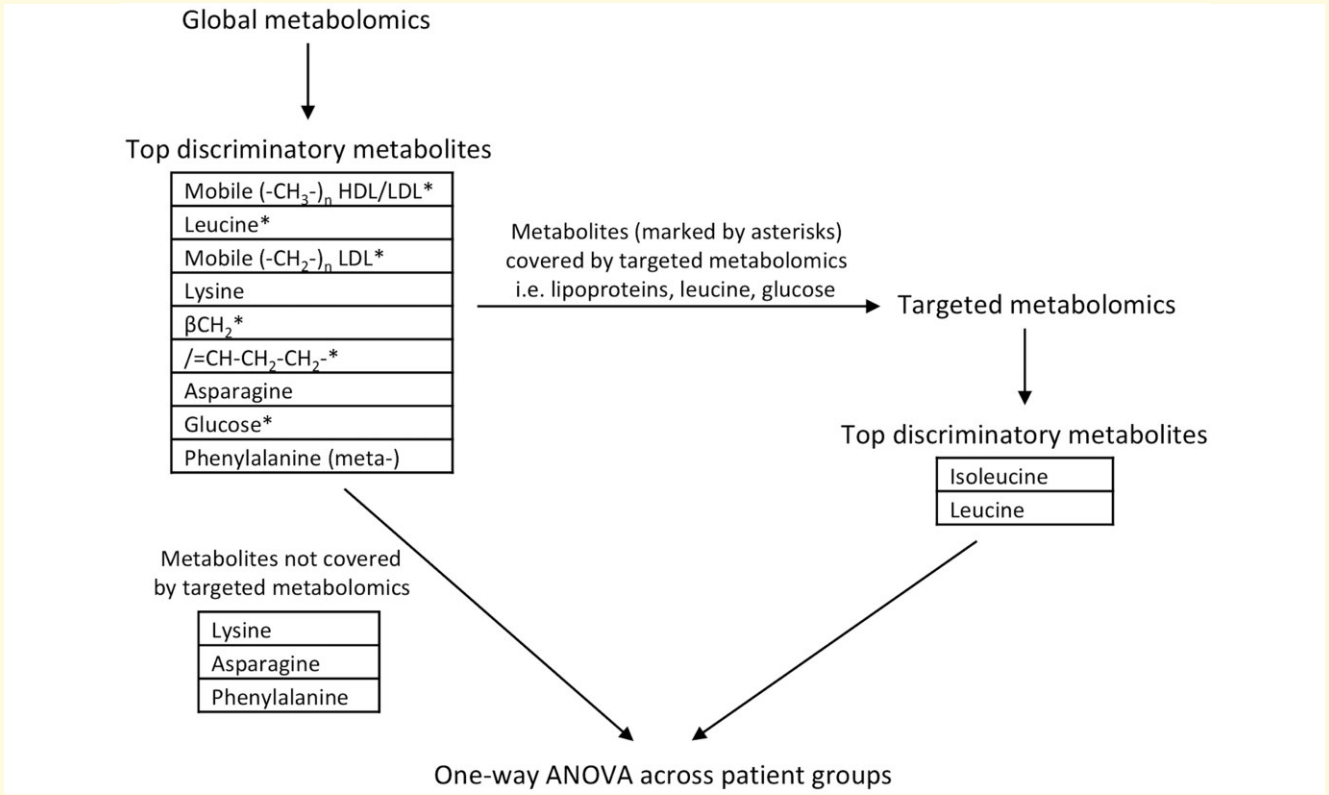

Figure 3 Workflow illustrating the selection of metabolites for one-way ANOVA across the four patient groups. * indicates metabolites accessible for absolute quantification by targeted metabolomics. HDL = high-density lipoprotein; LDL = low-density lipoprotein.

cohort (7 steroid users versus 194 non-steroid users) and indeed within R patients (5 steroid users versus 33 non-steroid users). For DMT use, higher isoleucine levels were observed in DMT users (mean ± SD, 82.3 ± 25.6 µmol/l versus 72.8 ± 18.7 µmol/l; $P = 0.011$) across the entire cohort (125 DMT users versus 76 non-DMT users). However, no differences in isoleucine levels were observed between DMT users and non-users within R patients (18 DMT users versus 20 non-DMT users) ($P = 0.120$) as well as within LR ≥ 24 M patients (75 DMT users versus 26 non-DMT users) ($P = 0.304$). There were also no significant associations/correlations of the discriminatory metabolites with smoking status, alcohol intake, body mass index and time from last meal.

Exploring associations of metabolite biomarkers with MRI indices of inflammatory activity

The associations of the identified metabolite biomarkers with MRI indices of inflammation, i.e. the presence of GAD-enhancing lesion/s or new T_2 lesion/s (referenced to baseline scan done ≤ 1 year apart) within the last 1 year were explored in the entire cohort. Lysine (mean ± SD, $25.5 \times 10^{-4} \pm 2.1 \times 10^{-4}$ AU versus $23.7 \times 10^{-4} \pm 2.4 \times 10^{-4}$ AU; $P = 0.008$) and asparagine (mean ± SD, $9.6 \times 10^{-4} \pm 1.2 \times 10^{-4}$ AU versus $8.9 \times 10^{-4} \pm 1.2 \times 10^{-4}$ AU; $P = 0.048$) levels were significantly higher in patients who had GAD-enhancing lesions. However, this association was not observed for isoleucine ($P = 0.074$) and leucine ($P = 0.231$). There were also no differences in the metabolite levels stratified by the presence of new T_2 lesion/s.

Discussion

The results from this study illustrate that (i) metabolic perturbations are present in patients during relapses as detected by global and targeted metabolomics, compared to patients without relapses for the past 2 years, and the summative magnitude of these perturbations decreased with time away from relapse; (ii) the four discriminatory metabolites that were significant on ANOVA (lysine, asparagine, isoleucine and leucine) across the different patient groups showed a consistent trend (either increasing or decreasing) with time away from relapse, and (iii) these metabolites are discriminatory in an individualized manner within a clinically useful time frame. Taken together, the results presented

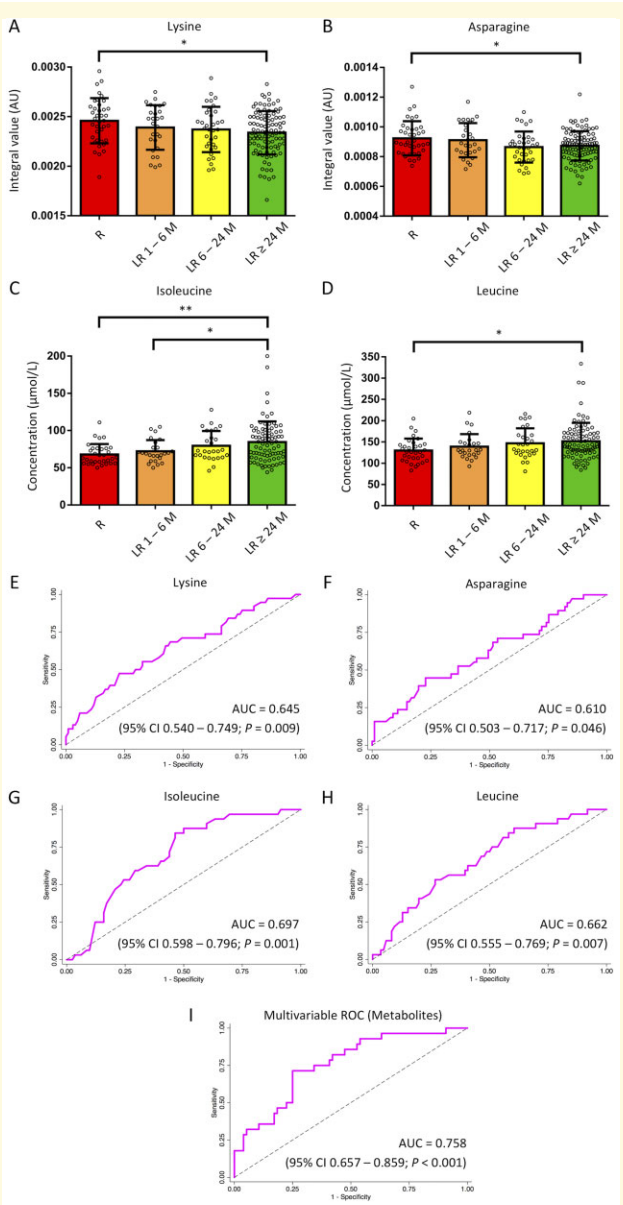

Figure 4 Discriminatory abilities of the identified metabolites at group level. (**A–D**) Significant metabolites on one-way ANOVA. Lysine and asparagine levels were higher within R patients compared to LR ≥ 24 M patients and decreased with time away from relapse. In contrast, isoleucine and leucine concentrations were lower during relapses and increased with time away from relapse. ** indicates $P < 0.01$ and * indicates $P < 0.05$ by *post-hoc* Holm–Sidak test, with LR ≥ 24 M patients as the reference comparator. (**E–H**) Univariable ROC analysis of the four metabolite biomarkers in distinguishing R versus LR ≥ 24 M patients. (**I**) Multivariable ROC analysis of the four metabolites. AU = arbitrary units; AUC = area under the curve; 95% CI = 95% confidence interval; LR 1–6 M = last relapse ≥ 1 month to < 6 months ago; LR 6–24 M = last relapse ≥ 6 months to < 24 months ago; LR ≥ 24 M = last relapse ≥ 24 months ago; R = in relapse; ROC = receiver operating characteristics.

here show that the use of a small set of blood-borne metabolites could identify relapses to facilitate optimal clinical management decisions.

The intra-individual differences of the four metabolite biomarkers in relapse versus in remission within a 6-month period is likely due to the dynamic nature of metabolic perturbations produced by the summative effects of various immunopathological processes that are amplified during relapses: (i) activation of peripheral T-cells and monocytes, and their subsequent access into the CNS; (ii) activation of resident microglial and astrocytes; (iii) initiation of injurious effector mechanisms leading to the production of reactive oxygen/nitrogen species and mitochondrial stress; and (iv) demyelination with possible axonal injury.[26] Although most of these pathophysiological processes occur within the CNS, it is not unexpected that metabolic perturbations can be detected in blood. Two possible explanations can account for this observation: (i) CNS metabolites involved in or resulting from these pathophysiological processes can move across an inflamed, leaky blood brain barrier[27]; and/or (ii) the metabolic perturbations are contributed mostly by peripheral processes, i.e. the activation of peripheral immune cells as well as the peripheral response to CNS injury, which, is mediated primarily by the liver.[28,29]

Concentrations of the BCAAs, isoleucine and leucine, were observed to be lower during relapses in this study. This is in agreement with another ^{1}H NMR metabolomics study demonstrating lower CSF isoleucine and valine in relapse compared to remission in multiple sclerosis patients, although discriminatory indices, such as AUC, were not provided.[19] Other metabolomics studies (both on ^{1}H NMR and mass spectrometry) have also reported that BCAAs are low in the plasma and the CSF of multiple sclerosis patients.[30,31] BCAAs are essential amino acids, which play roles in immune function and energy homeostasis. It has been shown that leucine, being an activator of the mammalian target of rapamycin (mTOR) complex 1, is involved in T-cell activation.[32] Additionally, a pro-inflammatory state as seen in multiple sclerosis is characterized by a marked increase in demand for substrates by activated immune cells, especially those required for energy and protein production.[29] Human immune cells express branched-chain aminotransferase and branched-chain α-ketoacid dehydrogenase, which, can metabolize BCAAs for these purposes.[33] Thus, the lower concentrations of isoleucine and leucine observed during multiple sclerosis relapses may reflect a consumptive deficiency as a result of these catabolic processes.

Lysine concentrations were observed to be elevated during relapses. This is consistent with observations in the myelin basic protein (MBP)-induced experimental autoimmune encephalomyelitis (EAE) model showing raised lysine in both CSF and intact CNS tissues using mass spectrometry and ^{1}H NMR spectroscopy techniques.[34,35] The putative role of lysine, an essential amino acid, within the context of multiple sclerosis pathogenesis is less clear although it is considered to be involved in the entry of arginine into leucocytes and thus on nitric oxide metabolism.[34] It is interesting to note that lysine is a

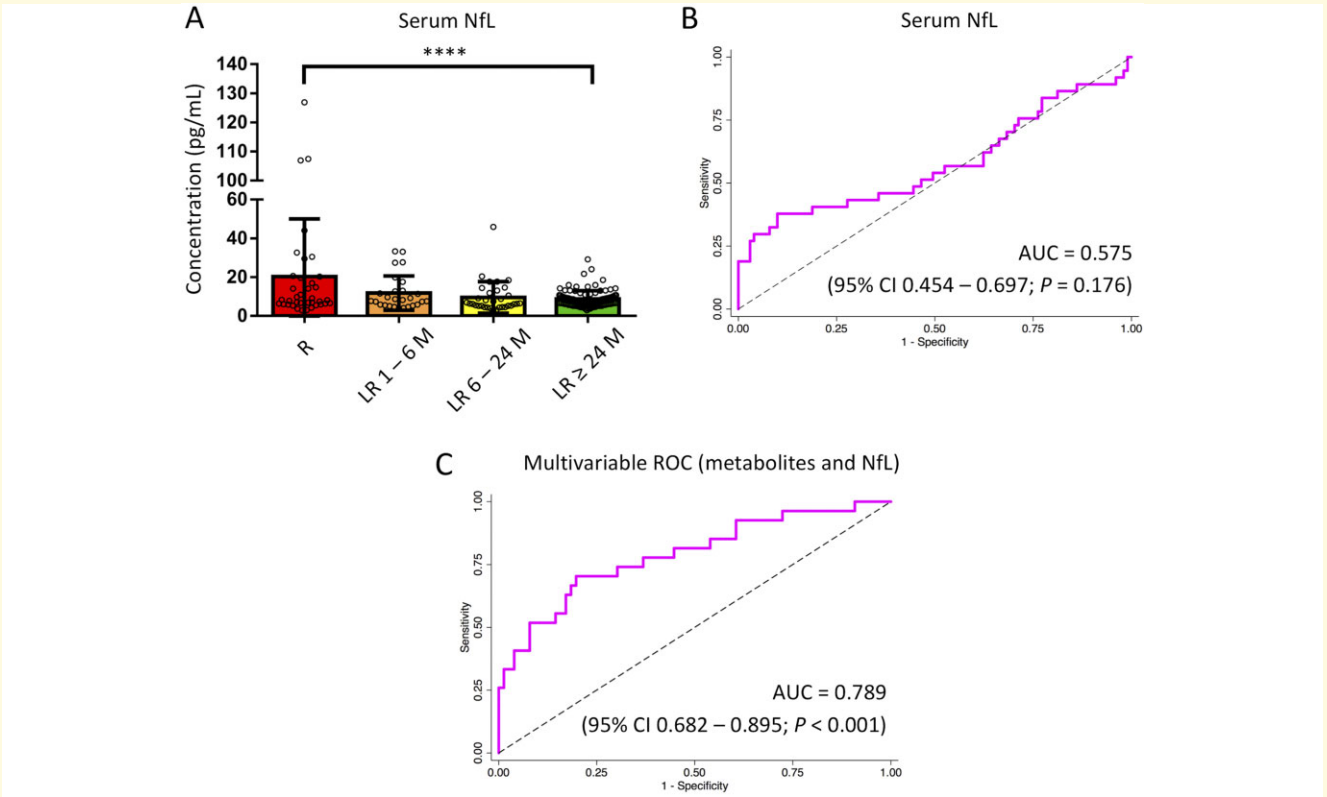

Figure 5 Discriminatory ability of serum NfL at group level. (**A**) One-way ANOVA showed that R patients had higher levels of serum NfL compared to LR ≥ 24 M patients. **** indicates $P < 0.0001$ by *post-hoc* Holm–Sidak test, with LR ≥ 24 M patients as the reference comparator. (**B**) Univariable ROC analysis of serum NfL in distinguishing R versus LR ≥ 24 M patients. (**C**) Multivariable ROC analysis using a combination of lysine, asparagine, isoleucine, leucine and NfL. AUC = area under the curve; 95% CI = 95% confidence interval; LR 1–6 M = last relapse ≥ 1 month to < 6 months ago; LR 6–24 M = last relapse ≥ 6 months to < 24 months ago; LR ≥ 24 M = last relapse ≥ 24 months ago; NfL = neurofilament-light chain; R = in relapse; ROC = receiver operating characteristics.

component, together with alanine, tyrosine and glutamic acid, of the complex mixture of linear and random polypeptides that make up glatiramer acetate, originally synthesized to mimic MBP.[36] The use of glatiramer acetate is unlikely to be a confounder in this study as fewer R patients (6/38, 15.8%) were on glatiramer acetate compared to LR ≥ 24 M patients (25/101, 24.8%), and that if anything, would have reduced the discriminatory ability of lysine. Additionally, the concentrations of alanine, tyrosine and glutamic acid were not different for R versus LR ≥ 24 M patients.

Asparagine levels were noted to be higher during relapses. It has been reported that CSF asparagine is increased in the MBP-EAE model as well as in the plasma and CSF of multiple sclerosis patients (compared to healthy controls).[37–39] Asparagine is a non-essential amino acid and may have a role in proper immune functioning, although its exact involvement in multiple sclerosis pathogenesis is not as yet clear. Asparagine has been shown to be involved in the priming of mTOR complex 1 for activation and within the context of Salmonella infection, the deprivation of asparagine in media abolishes T-cell activation, T-cell blastogenesis and interleukin-2 secretion.[40,41]

The concentrations of some lipoprotein species (Table 2) were found to be altered on global metabolomics during relapses, which, is consistent with a mass spectrometry metabolomics study showing that multiple sclerosis relapses were characterized by alterations in fatty acid metabolism, along with arginine–proline and glutathione perturbations in CSF.[18] Another mass spectrometry metabolomics study also observed that various serum phosphatidylcholine/lysophosphatidylcholine species and arachidonic acid were the main discriminatory metabolites differentiating patients who had relapses from those without relapses during a 2-year study period.[42]

No confounders for the relationship between the identified metabolites and relapses were observed. Steroids (commonly prescribed as oral methylprednisolone for 3–5 days in the UK) are given to patients in relapse and there is potential for steroids to induce changes to glucose and lipid metabolism.[43,44] Only 5 of the 38 R patients received steroids prior to blood sampling and none were

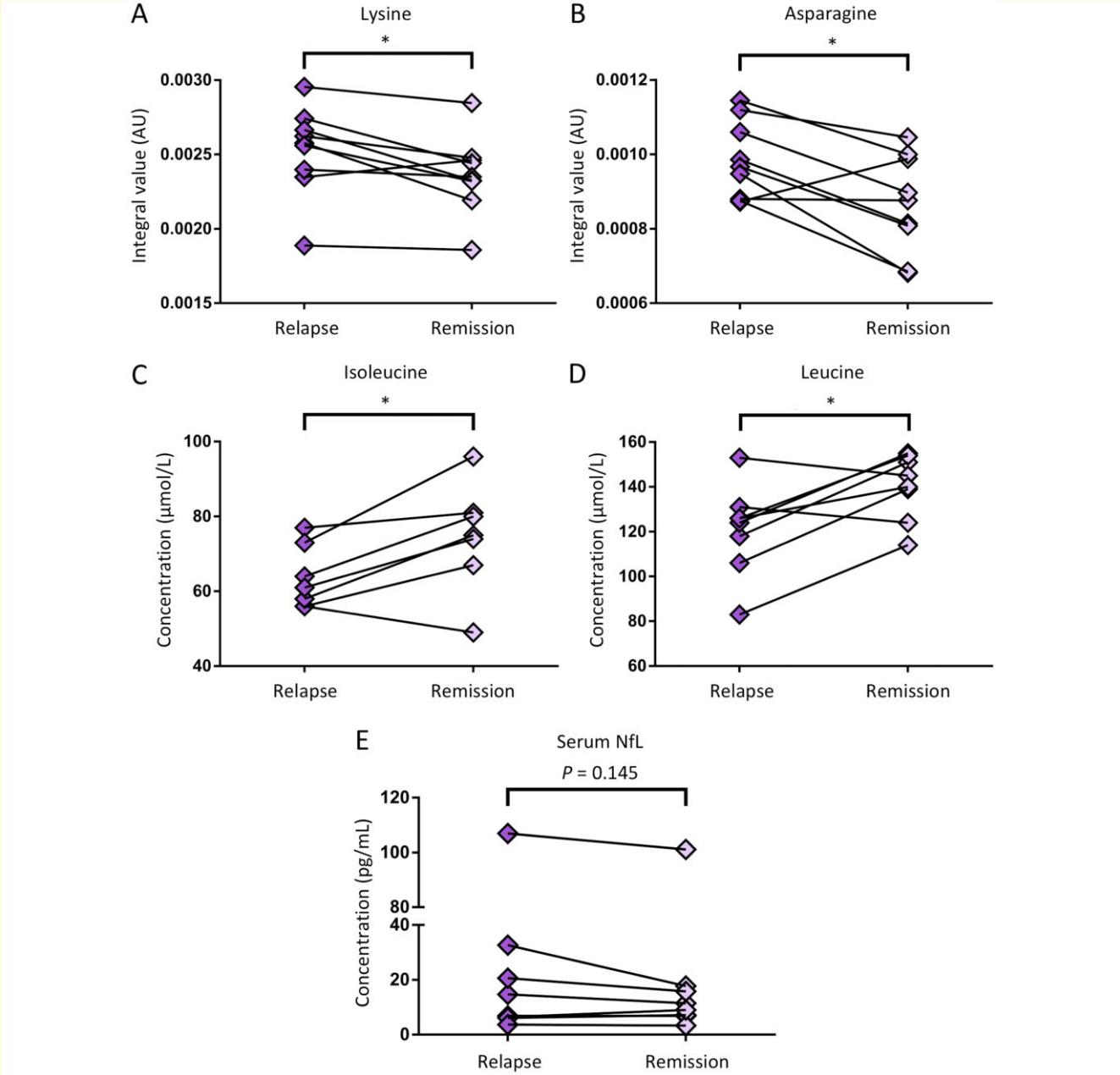

Figure 6 Discriminatory abilities of the identified metabolites and NfL at individual level. (**A–D**) Paired relapse–remission levels of the four metabolite biomarkers within individual patients. (**E**) Paired relapse–remission levels for serum NfL. * indicates $P < 0.05$ on paired *t*-test. For isoleucine, two patients had one missing data point, while for leucine, one patient had one missing data point, as the samples did not pass the quality control of the respective quantifier algorithms of the *AXINON*® *lipoFIT*® system. These patients were thus excluded from paired *t*-testing. AU = arbitrary units; NfL = neurofilament-light chain.

on steroids during sampling. Of note, targeted metabolomics (which measures predominantly lipid parameters and also glucose) showed that there was no difference between LR 1–6 M versus LR $\geq$ 24 M patients—the mean predictive accuracy of the OPLS-DA models was 51.7% ± 8.0% and was not statistically different from random chance ($P = 0.482$). This illustrates that the metabolic effects of short course, albeit high dose steroids are unlikely to persist in the longer term.

The pragmatic, observational nature of this study cohort meant that patients underwent MRI only when clinically indicated, which, would have reduced the detection of subclinical MRI-defined inflammation up till the point of relapse, especially for R patients. Additionally, a delay in presenting and then obtaining MRI meant that more GAD-enhancing and new T_2 lesions were seen in the 6 months after relapse. However, we focussed on clinical, not subclinical activity, and silent GAD-enhancing and

new T_2 lesions outside of a relapse are characteristics occurring around 10 times more frequently on MRI, thus, the differences we note may reflect this difference also. This could account for the fact that there were no associations between the four metabolites with the presence of new T_2 lesion/s, while only lysine and asparagine were associated with the presence of new GAD-enhancing lesion/s. Also, further analysis (not shown in the Results section) with the addition of MRI parameters, which, would theoretically increase the distinction between R versus LR $\geq$ 24 M patients did not result in higher accuracies—the mean predictive accuracy of OPLS-DA models of CPMG spectral data from R patients with presence of new GAD-enhancing lesion/s and/or new T_2 lesion/s (referenced to baseline scan done $\leq$1 year apart) in the next 6 months after relapse blood sampling ($n = 13$) versus LR $\geq$ 24 M patients with no new T_2 lesion/s (referenced to baseline scan done $\leq$1 year apart) in the last 1 year ($n = 19$) was only 58.6% $\pm$ 7.8%.

We have identified metabolites that appear to be able to distinguish multiple sclerosis patients in relapse from those downstream. Future metabolomics studies will need to prospectively include frequent MRI scans to understand metabolic signatures underlying subclinical MRI-defined inflammation and this may lead to the discovery of metabolite biomarkers to monitor disease activity that is independent of clinical relapses. Larger studies with regular metabolomics sampling involving more paired relapse–remission patients, and indeed remission–relapse patients, are also required to validate the predictive abilities of these candidate metabolites, which, may help to predict future relapses in an individualized manner to enable timely treatment escalation to obviate potential relapses. Additionally, objective assessment of clinical relapses using these metabolites would be useful in clinical trials and in monitoring DMT efficacy, and would add to our current diagnostic armamentarium as well as increase our understanding of the biology underlying the clinical expression of inflammation in multiple sclerosis.

Acknowledgements

The authors thank the Oxford Radcliffe Biobank for providing biobanking governance and support. This work received research support from numares AG for targeted metabolomics.

Funding

T.Y. is supported by the Ministry of Health, Singapore through the National Medical Research Council Research Training Fellowship (NMRC/Fellowship/0038/2016). F.P. is supported by the Medical Research Council (MC_PC_15029).

Competing interests

M.S., L.S., R.G., T.D.W.C., G.D., J.K. and J.P. report no competing interests relevant to the manuscript. T.Y. and F.P. have a pending UK provisional patent related to the findings arising from this study. S.H. and E.S. are employees of numares AG. D.L. is the CEO of GeNeuro. D.C.A. reports personal fees from Merck Serono Ltd and Novartis Pharmaceuticals UK Ltd during the conduct of the study and has a pending UK provisional patent related to the findings arising from this study.

References

1. Chard D, Trip SA. Resolving the clinico-radiological paradox in multiple sclerosis. *F1000Res*. 2017;6:1828.
2. Hickman SJ. Optic nerve imaging in multiple sclerosis. *J Neuroimaging*. 2007;17 (Suppl 1):42S–45S.
3. Kearney H, Miller DH, Ciccarelli O. Spinal cord MRI in multiple sclerosis–diagnostic, prognostic and clinical value. *Nat Rev Neurol*. 2015;11(6):327–338.
4. Martin SJ, McGlasson S, Hunt D, Overell J. Cerebrospinal fluid neurofilament light chain in multiple sclerosis and its subtypes: A meta-analysis of case-control studies. *J Neurol Neurosurg Psychiatry*. 2019;90(9):1059–1067.
5. Novakova L, Zetterberg H, Sundstrom P, et al. Monitoring disease activity in multiple sclerosis using serum neurofilament light protein. *Neurology*. 2017;89(22):2230–2237.
6. Thebault S, Abdoli M, Fereshtehnejad SM, Tessier D, Tabard-Cossa V, Freedman MS. Serum neurofilament light chain predicts long term clinical outcomes in multiple sclerosis. *Sci Rep*. 2020; 10(1):10381.
7. Akgun K, Kretschmann N, Haase R, et al. Profiling individual clinical responses by high-frequency serum neurofilament assessment in MS. *Neurol Neuroimmunol Neuroinflamm*. 2019;6(3):e555.
8. Huss A, Senel M, Abdelhak A, et al. Longitudinal serum neurofilament levels of multiple sclerosis patients before and after treatment with first-line immunomodulatory therapies. *Biomedicines*. 2020; 8(9):312.
9. Disanto G, Barro C, Benkert P, et al.; the Swiss Multiple Sclerosis Cohort Study Group. Serum Neurofilament light: A biomarker of neuronal damage in multiple sclerosis. *Ann Neurol*. 2017;81(6): 857–870.
10. Lin TY, Vitkova V, Asseyer S, et al. Increased serum neurofilament light and thin ganglion cell-inner plexiform layer are additive risk factors for disease activity in early multiple sclerosis. *Neurol Neuroimmunol Neuroinflamm*. 2021;8(5):e1051.
11. Tavazzi E, Jakimovski D, Kuhle J, et al. Serum neurofilament light chain and optical coherence tomography measures in MS: A longitudinal study. *Neurol Neuroimmunol Neuroinflamm*. 2020;7(4):e737.
12. Trivedi DK, Hollywood KA, Goodacre R. Metabolomics for the masses: The future of metabolomics in a personalized world. *New Horiz Transl Med*. 2017;3(6):294–305.
13. Jurynczyk M, Probert F, Yeo T, et al. Metabolomics reveals distinct, antibody-independent, molecular signatures of MS, AQP4-antibody and MOG-antibody disease. *Acta Neuropathol Commun*. 2017; 5(1):95.
14. Yeo T, Probert F, Jurynczyk M, et al. Classifying the antibody-negative NMO syndromes: Clinical, imaging, and metabolomic modeling. *Neurol Neuroimmunol Neuroinflamm*. 2019;6(6):e626.
15. Probert F, Yeo T, Zhou Y, et al. Integrative biochemical, proteomics and metabolomics cerebrospinal fluid biomarkers predict clinical conversion to multiple sclerosis. *Brain Commun*. 2021;3(2): fcab084.

16. Yeo T, Sealey M, Zhou Y, et al. A blood-based metabolomics test to distinguish relapsing-remitting and secondary progressive multiple sclerosis: Addressing practical considerations for clinical application. *Sci Rep*. 2020;10(1):12381.
17. Dickens AM, Larkin JR, Griffin JL, et al. A type 2 biomarker separates relapsing-remitting from secondary progressive multiple sclerosis. *Neurology*. 2014;83(17):1492–1499.
18. Park SJ, Jeong IH, Kong BS, et al. Disease type- and status-specific alteration of CSF metabolome coordinated with clinical parameters in inflammatory demyelinating diseases of CNS. *PLoS One*. 2016;11(11):e0166277.
19. Kim HH, Jeong IH, Hyun JS, Kong BS, Kim HJ, Park SJ. Metabolomic profiling of CSF in multiple sclerosis and neuromyelitis optica spectrum disorder by nuclear magnetic resonance. *PLoS One*. 2017;12(7):e0181758.
20. Thompson AJ, Banwell BL, Barkhof F, et al. Diagnosis of multiple sclerosis: 2017 revisions of the McDonald criteria. *Lancet Neurol*. 2018;17(2):162–173.
21. Wishart DS, Feunang YD, Marcu A, et al. HMDB 4.0: The human metabolome database for 2018. *Nucleic Acids Res*. 2018;46(D1): D608–D617.
22. Stratmann B, Krepak Y, Schiffer E, et al. Beneficial metabolic effects of duodenal jejunal bypass liner for the treatment of adipose patients with type 2 diabetes mellitus: Analysis of responders and non-responders. *Horm Metab Res*. 2016;48(10):630–637.
23. Baumstark D, Pagel P, Eiglsperger J, Pfahlert V, Huber F. NMR spectroscopy—a modern analytical tool for serum analytics of lipoproteins and metabolites. *LaboratoriumsMedizin*. 2015;38(3):137.
24. R Core Team. *R: A language and environment for statistical computing*. Vienna: R Foundation for Statistical Computing; 2013.
25. Thevenot EA, Roux A, Xu Y, Ezan E, Junot C. Analysis of the human adult urinary metabolome variations with age, body mass index, and gender by implementing a comprehensive workflow for univariate and OPLS statistical analyses. *J Proteome Res*. 2015; 14(8):3322–3335.
26. Dendrou CA, Fugger L, Friese MA. Immunopathology of multiple sclerosis. *Nat Rev Immunol*. 2015;15(9):545–558.
27. Alvarez JI, Cayrol R, Prat A. Disruption of central nervous system barriers in multiple sclerosis. *Biochim Biophys Acta*. 2011; 1812(2):252–264.
28. Anthony DC, Couch Y, Losey P, Evans MC. The systemic response to brain injury and disease. *Brain Behav Immun*. 2012; 26(4):534–540.
29. Pearce EL, Pearce EJ. Metabolic pathways in immune cell activation and quiescence. *Immunity*. 2013;38(4):633–643.
30. Kasakin MF, Rogachev AD, Predtechenskaya EV, Zaigraev VJ, Koval VV, Pokrovsky AG. Targeted metabolomics approach for identification of relapsing-remitting multiple sclerosis markers and evaluation of diagnostic models. *Medchemcomm*. 2019;10(10): 1803–1809.
31. Podlecka-Piętowska A, Kacka A, Zakrzewska-Pniewska B, et al. Altered cerebrospinal fluid concentrations of hydrophobic and hydrophilic compounds in early stages of multiple sclerosis-metabolic profile analyses. *J Mol Neurosci*. 2019;69(1):94–105.
32. Ananieva EA, Powell JD, Hutson SM. Leucine metabolism in T cell activation: MTOR signaling and beyond. *Adv Nutr*. 2016; 7(4):798S–805S.
33. Brosnan JT, Brosnan ME. Branched-chain amino acids: Enzyme and substrate regulation. *J Nutr*. 2006;136 (Suppl 1): 207S–211S.
34. Blanchet L, Smolinska A, Attali A, et al. Fusion of metabolomics and proteomics data for biomarkers discovery: Case study on the experimental autoimmune encephalomyelitis. *BMC Bioinformatics*. 2011;12:254.
35. Battini S, Bund C, Moussallieh FM, Çiçek AE, De Sèze J, Namer IJ. Metabolomics approaches in experimental allergic encephalomyelitis. *J Neuroimmunol*. 2018;314:94–100.
36. Scott LJ. Glatiramer acetate: A review of its use in patients with relapsing-remitting multiple sclerosis and in delaying the onset of clinically definite multiple sclerosis. *CNS Drugs*. 2013;27(11): 971–988.
37. Noga MJ, Dane A, Shi S, et al. Metabolomics of cerebrospinal fluid reveals changes in the central nervous system metabolism in a rat model of multiple sclerosis. *Metabolomics*. 2012;8(2): 253–263.
38. Poddighe S, Murgia F, Lorefice L, et al. Metabolomic analysis identifies altered metabolic pathways in Multiple Sclerosis. *Int J Biochem Cell Biol*. 2017;93:148–155.
39. Barkhatova VP, Zavalishin IA, Askarova L, Shavratskii V, Demina EG. Changes in neurotransmitters in multiple sclerosis. *Neurosci Behav Physiol*. 1998;28(4):341–344.
40. Torres A, Luke JD, Kullas AL, et al. Asparagine deprivation mediated by *Salmonella asparaginase* causes suppression of activation-induced T cell metabolic reprogramming. *J Leukoc Biol*. 2016; 99(2):387–398.
41. Dyachok J, Earnest S, Iturraran EN, Cobb MH, Ross EM. Amino acids regulate mTORC1 by an obligate two-step mechanism. *J Biol Chem*. 2016;291(43):22414–22426.
42. Villoslada P, Alonso C, Agirrezabal I, et al. Metabolomic signatures associated with disease severity in multiple sclerosis. *Neurol Neuroimmunol Neuroinflamm*. 2017;4(2):e321.
43. Pranger IG, van Raalte DH, Brands M, et al. Influence of prednisolone on parameters of de novo lipogenesis and indices for stearoyl-CoA- and Delta6- desaturase activity in healthy males: A post-hoc analysis of a randomized, placebo-controlled, double-blind trial. *Prostaglandins Leukot Essent Fatty Acids*. 2018;132: 8–15.
44. Bordag N, Klie S, Jurchott K, et al. Glucocorticoid (dexamethasone)-induced metabolome changes in healthy males suggest prediction of response and side effects. *Sci Rep*. 2015;5:15954.